

DRAFT VERSION DECEMBER 25, 2020

Typeset using L^AT_EX preprint style in AASTeX63

Is Dark Matter Light?

LORNE W HOFSTETTER¹

¹*Department of Radiology and Imaging Sciences, University of Utah, Salt Lake City, UT.*

ABSTRACT

Elucidating the nature of dark matter in galactic systems remains one of the important unsolved mysteries of modern cosmology. As a thought experiment, we consider a galaxy model where the light radiating outward from stellar objects produces a gravitational effect larger than Einstein's theory of gravity predicts. Using computer simulations, we observe that this assumption allows the basic rotation curve profiles observed in both dwarf and late-type spiral galaxies to be recreated. It is important to highlight that a separate mass model describing the dark matter halo is not needed or used. This toy model may also lead to insights about the nature of dark energy. If the gravitational effects in the universe are currently dominated by radiated light as this toy model may suggest, the cosmic scale factor would be closely linked to the time-history and spatial distribution of star formation and death rates. An accelerating universe may simply be a manifestation of star death rates exceeding star formation rates in the current epoch.

Keywords: dark matter, galaxy kinematics, rotation curves, Milky Way dark matter halo, cosmology, dark energy

1. INTRODUCTION

Nearly a century has passed since Oort and Zwickey first reported the presence of significant amounts of nonluminous matter in two gravitational systems (Trimble 1987). More recently, the analysis of galaxy clusters and the rotation speed of spiral galaxies (Einasto et al. 1974; Ostriker et al. 1974; Rubin et al. 1985) have definitively shown that this nonluminous matter (i.e. dark matter) is ubiquitous. As a general trend, the mass of galactic systems tends to increase linearly with radius out to tens of kiloparsecs even though the density of observed stars decreases dramatically at such distances.

Numerous dark matter candidates (Trimble 1987; Bahcall 2015) and new theories of gravity (Milgrom 1983; Farnes 2018) have been proposed to explain this phenomenon. However, despite these continued efforts, the nature of dark matter is still widely questioned and sought after. In what follows we undertake a simple thought experiment that may provide insights about the composition of dark matter.

In Newtonian physics, an object's inertial mass and gravitational mass are assumed equivalent. This mass equality is essential when using Newton's second law and Newton's law of gravity to show

Corresponding author: Lorne W Hofstetter
lorne.hofstetter@hsc.utah.edu

the Weak Equivalence Principle (WEP). Namely, that the acceleration of an object in a uniform gravitational field is independent of the objects mass and composition (Poisson & Will 2014). Without affecting the WEP as it applies to matter with a non-zero rest mass, we consider Newtonian galaxy models where the photon is allowed to have a certain gravitational mass. In short, we suppose that photons emitted by stellar objects in the galaxy create a gravitational effect that is significantly larger than the effect predicted by Einstein's theory of gravity.

Using stationary galaxy simulations, we characterize the impact of the photon gravitational mass on the circular speed profiles. Using this model, basics rotation curve dynamics observed in dwarf galaxies and late-type spiral galaxies can be recapitulated. It is important to emphasize that the simulated galaxy models do not include a traditional dark matter halo component. These findings may suggest one of the following: (1) the current theory of gravity needs modification, or (2) the missing mass in a galaxy follows a distribution that closely matches the distribution of photons radiated by it's stellar objects.

2. PRELIMINARIES

Using a Newtonian perspective of gravity, we consider a galaxy model with a total gravitational mass density of

$$\rho(\vec{x}) = \rho_m(\vec{x}) + \rho_L(\vec{x}), \quad (1)$$

where $\rho_m(\vec{x})$ is the gravitational mass density of light-emitting matter (i.e. stellar mass density) and $\rho_L(\vec{x})$ is the gravitational mass density of the radiated photons. For simplicity, we consider the case where all light-emitting matter has a constant mass-to-light ratio of Υ and photons are radiated isotropically with a wavelength that corresponds to the peak wavelength of a radiating black body at temperature T . Using these assumptions, the number density of radiated photons (photons radiated per unit time per volume) can be written as

$$n(\vec{x}) = \frac{b}{\Upsilon hcT} \rho_m(\vec{x}), \quad (2)$$

where h is Planck's constant, c is the speed of light, and b is Wein's displacement constant.

Using the geometry depicted in Figure 1, the photon number density (photons per volume) at position \vec{x} due to photons radiated isotropically from position \vec{x}_1 is given by

$$N(\vec{x}, \vec{x}_1) = \frac{n(\vec{x}_1)}{4\pi c |\vec{x} - \vec{x}_1|^2}. \quad (3)$$

The total photon number density at \vec{x} can be calculated by integrating Equation (3) and substituting the result from Equation (2) to get

$$N(\vec{x}) = \frac{b}{4\pi c^2 \Upsilon h T} \iiint_V \frac{\rho_m(\vec{x}_1)}{|\vec{x} - \vec{x}_1|^2} d\vec{x}_1, \quad (4)$$

where V is a volume containing all light-emitting matter in the galaxy. Multiplying this result by the photon gravitational mass m_L gives the photon gravitational mass density

$$\rho_L(\vec{x}) = m_L N(\vec{x}) = \frac{K}{4\pi} \iiint_V \frac{\rho_m(\vec{x}_1)}{|\vec{x} - \vec{x}_1|^2} d\vec{x}_1 \quad (5)$$

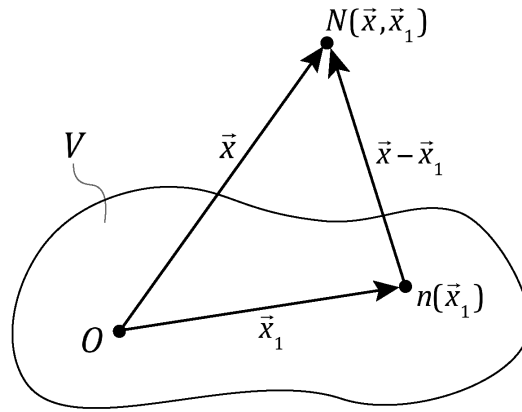


Figure 1. Geometry used to determine the photon number density $N(\vec{x}, \vec{x}_1)$ at \vec{x} due to isotropically radiated photons from a source at \vec{x}_1 .

where K is the constant scaling terms defined by

$$K = \frac{m_L b}{c^2 \Upsilon h T}. \quad (6)$$

Thus, if the luminous mass density is known, the total photon gravitational mass density generated by the light-emitting mass in a galaxy can be computed using Equations (5) and (6).

A few preliminary results from Chapter 2 of Binney and Tremaine (Binney & Tremaine 2008) that will be useful in later sections are summarized here. For systems with spherical symmetry, the circular speed can be obtained by applying Newton's first and second theorems—namely if $M(r)$ is the total gravitational mass enclosed within a spherical shell of radius r , the circular speed at r is given by

$$v_c(r) = \sqrt{\frac{GM(r)}{r}}. \quad (7)$$

For an arbitrary mass density $\rho(\vec{r})$ the Newtonian gravitational potential can be computed using the integral form of Poisson's equation

$$\Phi(\vec{x}) = -G \iiint_V \frac{\rho(\vec{x}_1)}{|\vec{x} - \vec{x}_1|} d\vec{x}_1, \quad (8)$$

where G is the gravitational constant, and the volume V is over all space where $\rho(\vec{x}) \neq 0$. The circular speed of a test object moving in the $z = 0$ plane located a distance R from the origin is given by

$$v_c(R, z = 0) = \sqrt{R \frac{\partial \Phi}{\partial R}}. \quad (9)$$

In the analysis that follows, geometrically simple galaxy models are used to demonstrate that models with a non-zero photon gravitational mass can recapitulate the flat rotation curve phenomenon that have been widely observed in spiral galaxies.

3. POINT SOURCE MODEL

Consider a point source of mass m having a mass-to-light ratio Υ and a black body temperature T . Using the Dirac delta function, the gravitational mass density can be written as $\rho_m(\vec{x}) = m\delta(\vec{x})$.

Using this expression and Equation (5), the photon gravitational mass density generated by photons emitted from the point source can be written as

$$\rho_L(\vec{r}) = \frac{Km}{4\pi r^2} \quad (10)$$

where K is the constant defined by Equation (6) and $r = |\vec{r}|$. The total photon gravitational mass contained within a spherical shell of radius r centered about the point source is given by

$$M_L(r) = 4\pi \int_0^r r'^2 dr' \rho_L(r') = Kmr \quad (11)$$

and the total gravitational mass within the shell is

$$M(r) = m + M_L(r) = m(1 + Kr). \quad (12)$$

Due to the spherical symmetry of the mass distribution, the circular speed can be calculated using Equations (12) and (7) to give

$$v_c(r) = \sqrt{Gm \left(\frac{1}{r} + K \right)}. \quad (13)$$

For small r the circular speed is dominated by the $1/\sqrt{r}$ term and follows the Keplerian speed profile. However, for large distances $v_c(r) \approx \sqrt{GmK}$ and the circular speed becomes constant and independent of radius. This simple point-source model suggests that the flat rotation curve dynamics can be modeled without the use of a dark matter halo component.

It is useful to define the transition distance r_o to be the radial distance at which the point mass and photon gravitational mass density contribute equally to the circular speed. Beyond this distance, the circular speed profile starts to flatten. From Equation (13) it can be shown that this transition distance is

$$r_o = \frac{1}{K} = \frac{c^2 \Upsilon h T}{m_L b}. \quad (14)$$

and depends on the photon gravitational mass m_L and the mass-to-light ratio Υ and the black body temperature T of the point source.

We can use Equation (14) and basic galaxy rotation curve properties to approximate a lower bound for the photon gravitational mass that would be needed to explain flat galaxy rotation curves. Rotation curves for late-type spiral galaxies tend to become flat at a radius between 2 to 8 kpc from the galactic center (Rubin et al. 1985). The rotation velocity for the Milky Way has a maximum around 5 kpc after which the curve is predominantly flat out to at least 20 kpc (Reid et al. 2014; Mróz et al. 2019). The Large Magellanic Cloud (a small Sb galaxy) has a broad velocity maximum somewhere between 2 - 7 kpc and is mostly flat beyond 7 kpc (Sofue 1999). Taken in combination, these observations suggest that rotation curves for a wide range of spiral galaxies tend to flatten at radial distances somewhere between 2 and 8 kpc—suggesting that the transition distance r_o is less than 8 kpc.

Figure 2 plots the relationship between the photon gravitational mass and transition distance for a point-source galaxy model where $\Upsilon = \Upsilon_\odot$ and $T = T_\odot$. The 8 kpc transition corresponds to a minimum photon gravitational mass of 1.5 Daltons. A transition distance closer to 3 kpc may be more realistic for many systems and corresponds to a photon gravitational mass of 4.0 Daltons.

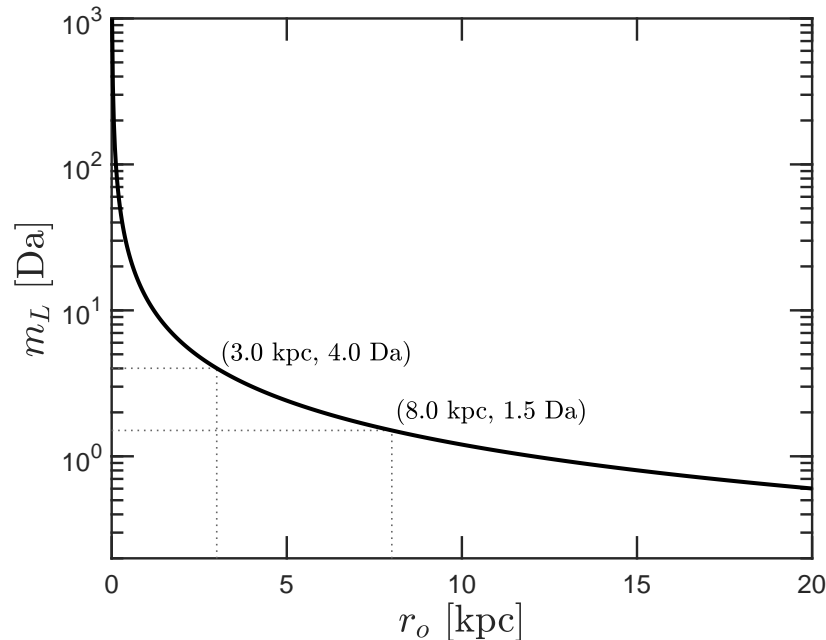


Figure 2. Photon gravitational mass as a function of transition distance for the point-source model where $T = T_{\odot}$ and $\Upsilon = \Upsilon_{\odot}$.

Next we use the point-source model to calculate the circular velocity profile for an object producing a total luminosity of $3.0 \times 10^{10} L_{\odot}$. This luminosity value was chosen to be equivalent to the Milky Way galaxy luminosity reported in Chapter 1 of Binney and Tremaine (Binney & Tremaine 2008). The circular velocity curves were calculated and plotted in Figure 3 for photon gravitational masses ranging from 0 to 6.5 Daltons. The model with $m_L = 4$ Daltons had a circular speed of 236, 222, and 213 km/s, at a radius of 10, 20 and 50 kpc, respectively, which is comparable to the measured flat rotation speed of the Milky Way (Reid et al. 2014; Mróz et al. 2019). The model in Figure 3 with $m_L = 0$ recovers the Keplerian behavior for a point source. For models where m_L is non-zero, the circular speed at large r increases for larger photon gravitational mass.

4. HOMOGENOUS SPHERE MODEL

Next we consider a homogeneous sphere galaxy model where the mass density of light-emitting matter is given by

$$\rho_m(r) = \begin{cases} \rho_o & \text{for } r \leq a_o \\ 0 & \text{for } r > a_o. \end{cases} \quad (15)$$

where a_o is the radius of the sphere, and ρ_o is a constant. We compute the photon gravitational mass density $\rho_L(\vec{x})$ by numerically evaluating the integral in Equation (5) using Fourier transform methods (see Appendix A for details). For the integration, a gridding of 1024 elements along each dimension in 3D space with a grid spacing of 50 pc results in the length of the integrated volume extending to ± 25.6 kpc along each axis. Since the gravitational mass density of matter and emitted photons are both spherically symmetric, circular velocity profiles can be computed using Equation (7).

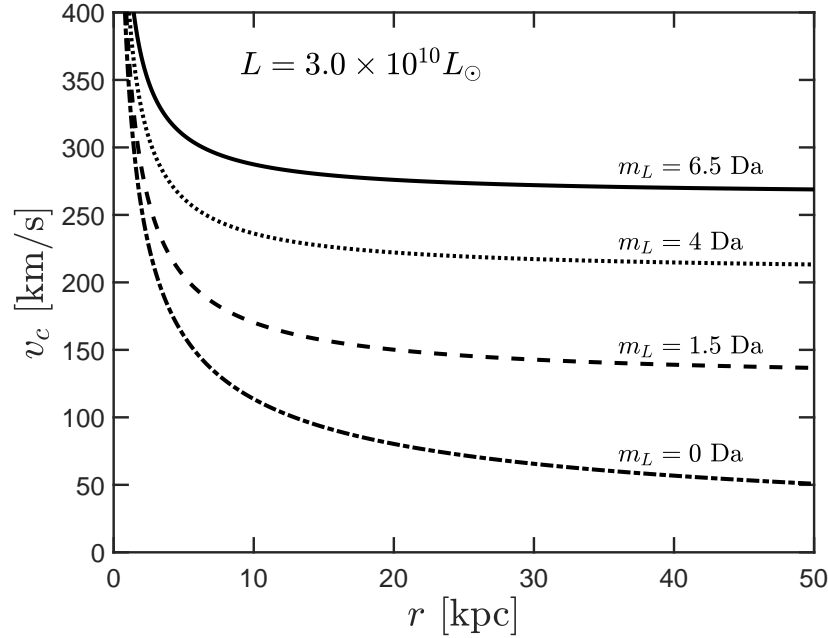


Figure 3. Circular velocity as a function of radius using point source model for galaxy having a total luminosity of $3.0 \times 10^{10} L_{\odot}$ where $T = T_{\odot}$ and $\Upsilon = \Upsilon_{\odot}$. Velocity curves were computed for photon gravitational masses of 0, 1.5, 4, and 6.5 Daltons.

The photon gravitational mass density and circular velocity profiles were calculated for four different galaxy models where a_o equal to 2, 5, 10 and 20 kpc, respectively. For all models the following parameters were used: $m_L = 4$ Daltons, $\Upsilon = \Upsilon_{\odot}$, $T = T_{\odot}$ and $\iiint_V \rho_m(\vec{x}) d\vec{x} = 3.0 \times 10^{10} M_{\odot}$.

Figure 4 plots the photon gravitational mass density as a function radius from the galactic center for each homogeneous spherical galaxy model. Although the total luminosity is the same for all models, a_o , which controls the spatial extent and density of the luminous matter, has a significant impact on the width and amplitude of the central core of $\rho_L(\vec{x})$. This difference is also reflected in the shape of the calculated circular speed profiles shown in Figure 5. This galaxy model, while geometrically simple, demonstrates that the structure and distribution of light-emitting matter in a galaxy ($\rho_m(\vec{x})$) will significantly impact the shape of the photon gravitational mass density ($\rho_L(\vec{x})$) and its contribution to the circular speed profile. For the more compact galaxy model, $a_o = 2$ kpc, the mass density of matter dominates the circular speed near the galactic center. However, for the more dispersed model, $a_o = 20$ kpc, the circular speed is dominated by the photon gravitational mass density at all radii.

5. MILKY WAY GALAXY MODEL

We use the mass models in Dehnen and Binney (Dehnen & Binney 1998) to model the bulge and disk of the Milky Way. The disk is assumed to have a thin, thick, and ISM component with a scale height (z_d) of 300, 1000, and 80 pc, respectively. R_m , which allows for a central depression in the ISM near the galactic center, is set to 4 kpc for the ISM and 0 for the thin and thick components of the disk. The relative mass of each component is determined by letting the thin, thick, and ISM components of the disk comprise 70%, 5%, and 20% of the surface-density at $R_o = 8.2$ kpc, respectively. The disk-scale length of the ISM is $2R_d$ where R_d is the disk-scale length of the thin and

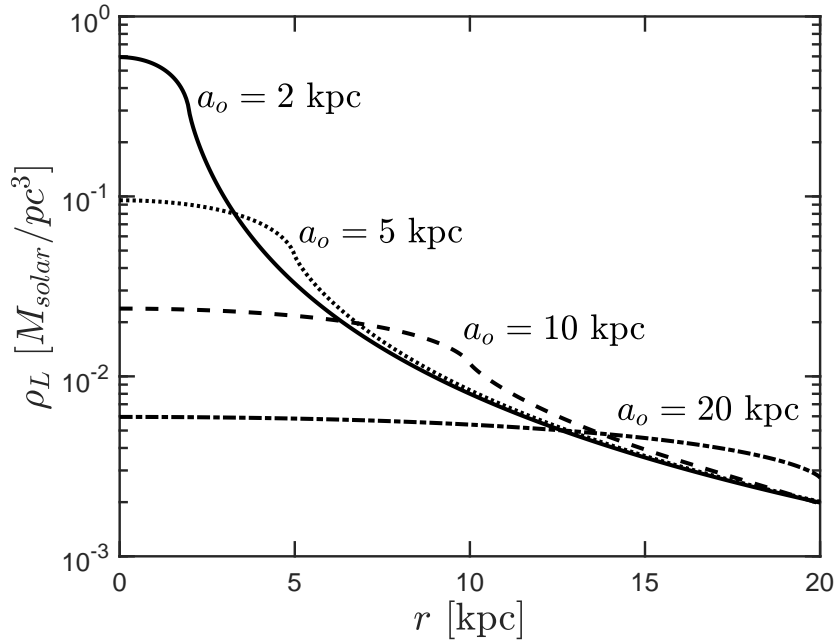


Figure 4. Photon gravitational mass density profiles for homogeneous sphere galaxy models where $a_0 = 2, 5, 10,$ and 20 kpc.

thick disk. The bulge geometry defined by the 4 parameter values provided in Dehnen and Binney (Dehnen & Binney 1998) is used. The bulge density is scaled by a constant factor so that the bulge has total mass of M_b . We do not include a separate spheroidal model of the dark matter halo density.

To determine the photon gravitational mass density, we assume that the thin and thick components in the disk and the bulge are comprised of a stellar population having the same mass-to-light ratio, Υ , and effective temperature, T . The wavelength of all emitted photons is assumed to be the peak wavelength emitted by a radiating black body of temperature T . The gravitational photon mass m_L is assumed nonzero. Any radiation from or extinction due to the ISM component of the disk is neglected. The total photon gravitational mass density produced from the light-emitting matter is computed numerically using Equation (5). Values for galaxy model parameters that have not been stated above are shown in Table 1.

The gravitational potential of the disk, bulge, and radiated photons are calculated by numerically integrating Equation (8) using the Fourier transform method. For all integrations, a gridding of 1280 elements along each dimension in 3D space with a grid spacing of 150 pc results in a total model length extending to ± 96 kpc in each dimension. The mass densities of the bulge and disk are well contained in this volume and calculation of the gravitational potential for each component is straightforward. However, calculation of the potential for the photon gravitational mass density is complicated by the fact that a non-negligible mass density extends beyond ± 96 kpc distances. Prior to numerical integration, the photon gravitational mass density was truncated by setting the density to zero for radial distances greater than 95.6 kpc. Using the computed gravitational potential, the circular speed in the galactic plane is found using Equation (9).

Truncation of the photon gravitational mass density can introduce errors in the calculated potential and circular speed profile. The magnitude of this error was evaluated using the spherical galaxy

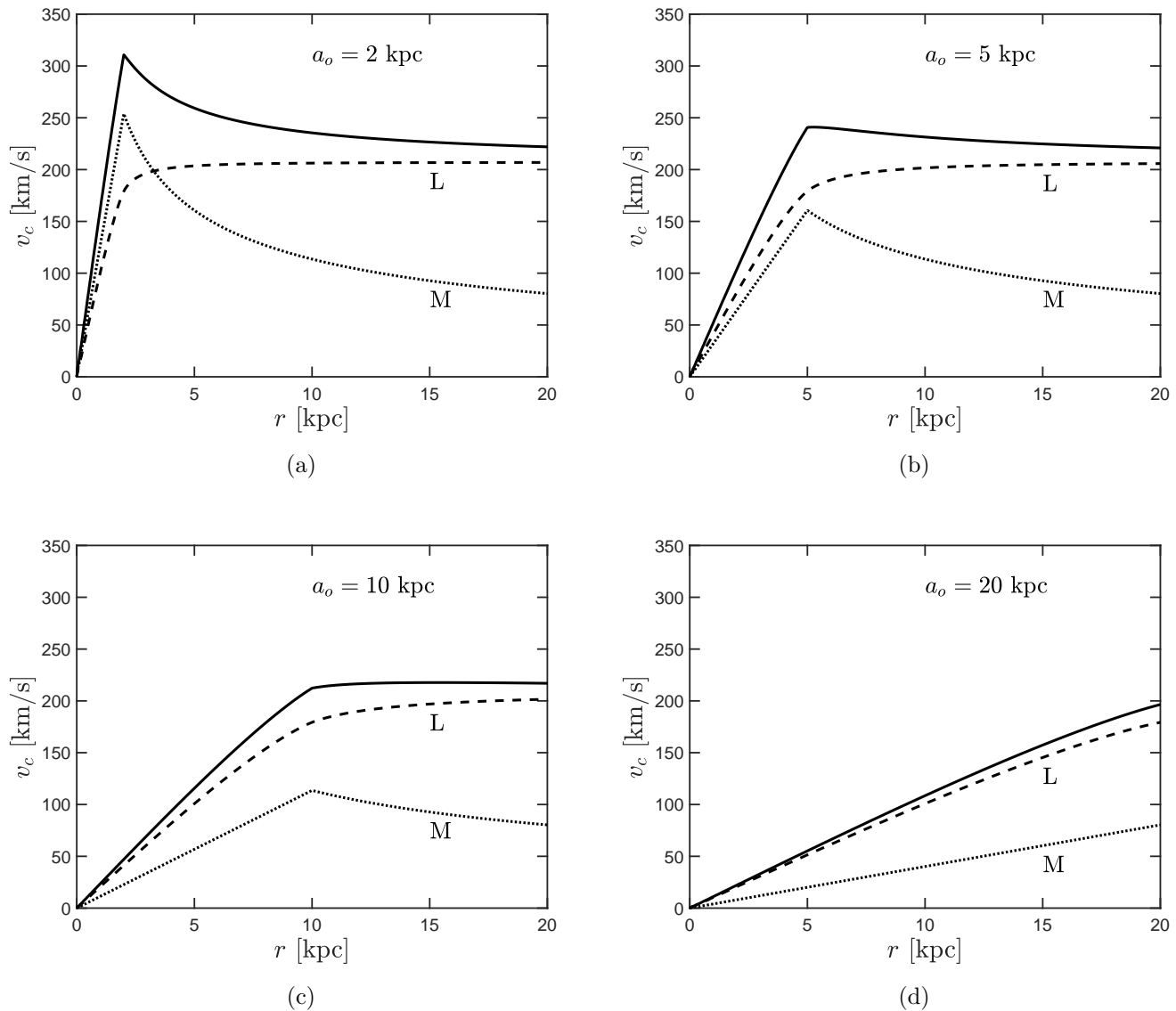


Figure 5. Circular speed curves for homogeneous sphere models are shown (solid line) for $a_o = 2, 5, 10,$ and 20 kpc. The dashed lines (L) denote the contribution from the photon gravitational mass density and the dotted lines (M) denote the contribution from the light-emitting mass density.

models in Section 4 since the circular speed of these symmetric systems can be accurately calculated using the spherical shell method of Equation (7). The same gridding and truncation distance used for the Milky Way Galaxy models was used to calculate the potential and resulting circular speed for each spherical galaxy model in Section 4. For distances less than 20 kpc from the galactic center, the root mean square deviation between the circular speed profiles computed using the potential method and spherical shell method was less than 1.41 km/s—suggesting that truncation of the photon gravitational mass density at 95.6 kpc has a relatively minor impact on the calculated circular speed for distances less than 20 kpc from the galactic center.

The circular speed curves for the two Milky Way Galaxy models are shown in Figure 6. For Model I, the maximum circular speed of 244 km/s occurs at 7.5 kpc from the galactic center and at 20 kpc

Table 1. Parameters of Milky Way Galaxy models

Parameter	Model I	Model II
R_d	2 kpc	2.5 kpc
M_d	$2.85 \times 10^{10} M_\odot$	$4.50 \times 10^{10} M_\odot$
M_b	$0.5 \times 10^{10} M_\odot$	$0.45 \times 10^{10} M_\odot$
L_{d+b}	$3.0 \times 10^{10} M_\odot$	$2.27 \times 10^{10} M_\odot$
Υ	$1 M_\odot/L_\odot$	$1.8 M_\odot/L_\odot$
m_L	4 Da	2.5 Da
T	5770 K	5770 K

NOTE— M_d and M_b are the total mass of the disk and bulge, respectively. L_{d+b} is the total luminosity of the disk and bulge.

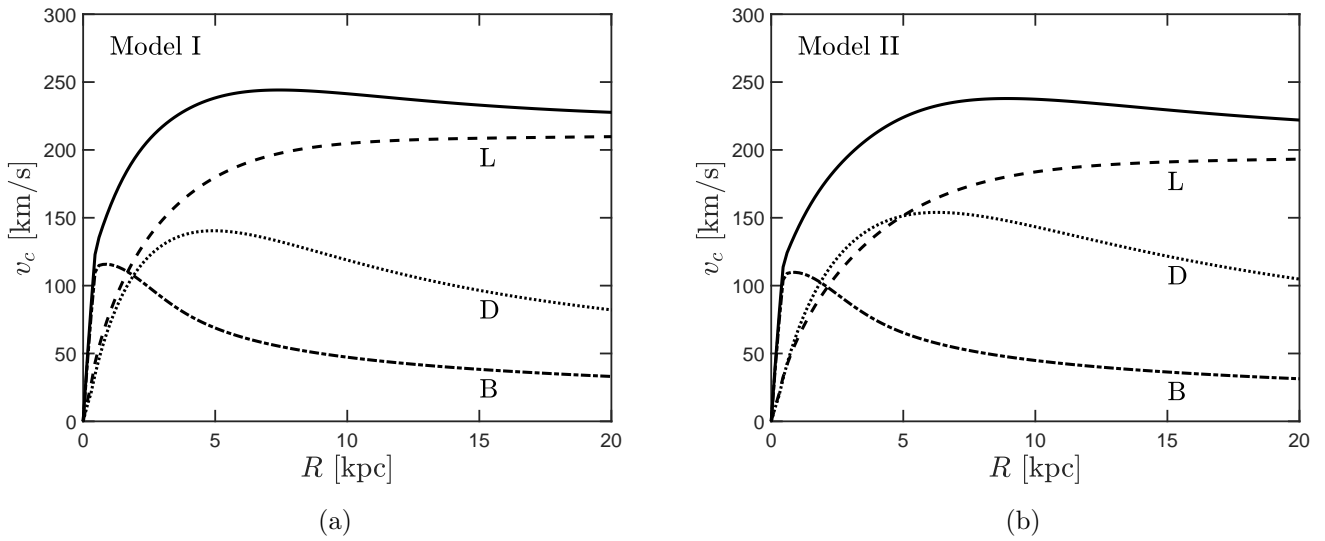


Figure 6. Simulated circular speed curve (solid line) in disk of Milky Way for Model I (a) and II (b). The dashed line (L) denotes the contribution from the photon gravitational mass density, the dotted line (D) is the contribution from the disk matter, and the dash-dot line (B) is the contribution from the bulge matter.

the speed falls to 228 km/s. For Model II, a maximum of 238 km/s occurs 9 kpc from the galactic center and at 20 kpc the speed is 222 km/s. The simulated circular speed curves of Model I and II are strikingly similar to the measured rotation curve for the Milky Way (Reid et al. 2014; Mróz et al. 2019). The models in Figure 6 only assume the existence of the disk and bulge components and a non-zero photon gravitational mass of 4 and 2.5 Daltons, respectively. Separate modeling of a dark matter halo component is not needed to obtain a circular speed curve shape that is characteristic of the Milky Way.

6. CONCLUSION & DISCUSSION

In this work we have examined galaxy models where photons radiated from stellar objects are assigned a gravitational mass that is on the order of the proton's mass. Using this assumption, the basic rotation curve characteristics of spiral galaxies can be recreated. Use of a separate ill-defined mass model for the 'dark matter' component does not appear to be necessary.

Such a model may also go towards explaining why the distribution and amount of dark matter can vary significantly among galaxies. Results from the homogeneous sphere models in Figure 4 show that the shape of the photon gravitational mass density critically depends on the distribution of luminous matter. For a dispersed model (Figure 5d), the photon gravitational mass dominates the circular speed profile at nearly all distances and the circular speed profile is increasing out to 20 kpc. Similar profile shapes are commonly seen in dwarf galaxies which tend to be dark matter dominated and exhibit rotation curves that increase with increasing distance from the galaxy center (de Blok et al. 2001; Sofue & Rubin 2001). For the most compact spherical galaxy model (Figure 5a), the photon gravitational mass only dominates the speed at distances larger than 3.3 kpc from the galactic center. This circular speed profile is more similar to the flat rotation curves seen in late-type galaxies (Sofue & Rubin 2001). Extinction from galactic dust, while not modeled in this work, could significantly alter the photon gravitational mass density shape as well. These factors among potentially others may give the model the flexibility needed to describe the wide range of circular speed profiles that have been measured in many different galaxies.

The toy model presented in this work may also offer insights into the nature of dark energy and observations by Riess et al. (Riess et al. 1998) and Perlmutter et al. (Perlmutter et al. 1999) of an accelerating universe. Since both stellar lifetimes and the age of the universe are finite, the photon gravitational mass density, on cosmic scales, will depend on the epoch and the time-history and spatial distribution of star formation and death rates. This time-dependent contribution to the total gravitational mass density would result in an additional contributor to the evolution of the cosmic scale factor.

The key concept used throughout this work assumes that photons radiated from stellar objects produce a significant gravitational effect. While this assumption ultimately may be incorrect, the ability of this construct to potentially model the distribution of dark matter in a variety of galaxy systems is quite striking and warrants further consideration. It is possible that dark matter is predominantly comprised of a different particle type whose spatial distribution in galaxies closely matches the distribution described by this radiating photon model.

ACKNOWLEDGMENTS

Many thanks to Victor Hofstetter for helpful discussions and useful comments.

APPENDIX

A. APPENDIX

Integrals in Equations (5) and (8) are equivalent to the convolution integral of the following form

$$(\rho * g)(\vec{x}) = \int_{\mathbb{R}^3} g(\vec{x}_1)\rho(\vec{x} - \vec{x}_1)d\vec{x}_1, \quad (\text{A1})$$

where,

$$g(\vec{x}) = \begin{cases} \frac{K}{4\pi|\vec{x}|^2} & \text{for Equation (5),} \\ -\frac{G}{|\vec{x}|} & \text{for Equation (8),} \end{cases} \quad (\text{A2})$$

and where $\rho(\vec{x})$ is the gravitational mass density. While $g(\vec{x})$ has a singularity at the origin, integration of $g(\vec{x})$ over a small spherical volume centered on the origin is finite for both expressions. Exploiting this property of the singularity and if the density $\rho(\vec{x})$ is well behaved and is non-zero over a finite volume, the integral in Equation (A1) can be approximated using the following discretized form

$$(\rho * g)(\vec{x}) = h^3 \sum_{n_x} \sum_{n_y} \sum_{n_z} \bar{g}(hn_x, hn_y, hn_z) \rho(x - hn_x, y - hn_y, z - hn_z) \quad (\text{A3})$$

where h is the isotropic step size of the discretization, and n_x , n_y , and n_z are integers specifying the location in the discretized gridding, and

$$\bar{g}(hn_x, hn_y, hn_z) = \begin{cases} \frac{1}{h^3} \int_{-h/2}^{h/2} \int_{-h/2}^{h/2} \int_{-h/2}^{h/2} g(x', y', z') dx' dy' dz' & \text{for } n_x = n_y = n_z = 0, \\ g(hn_x, hn_y, hn_z) & \text{otherwise.} \end{cases} \quad (\text{A4})$$

The right hand side of Equation (A3) is the discrete convolution of \bar{g} and ρ multiplied by a scaling term h^3 . Since both \bar{g} and ρ are finite the discrete convolution in the right hand side of Equation (A3) can be calculated using the discrete Fourier transform and convolution theorem (Gonzalez & Woods 2008).

REFERENCES

- Bahcall, N. A. 2015, Proceedings of the National Academy of Sciences, 112, 12243
- Binney, J., & Tremaine, S. 2008, Galactic Dynamics: Second Edition
- de Blok, W. J. G., McGaugh, S. S., Bosma, A., & Rubin, V. C. 2001, ApJL, 552, L23
- Dehnen, W., & Binney, J. 1998, MNRAS, 294, 429
- Einasto, J., Kaasik, A., & Saar, E. 1974, Nature, 250, 309
- Farnes, J. S. 2018, A&A, 620, A92
- Gonzalez, R., & Woods, R. 2008, Digital Image Processing (Pearson Education Inc.)
- Milgrom, M. 1983, ApJ, 270, 365
- Mróz, P., Udalski, A., Skowron, D. M., et al. 2019, The Astrophysical Journal, 870, L10
- Ostriker, J. P., Peebles, P. J. E., & Yahil, A. 1974, ApJL, 193, L1
- Perlmutter, S., Aldering, G., Goldhaber, G., et al. 1999, The Astrophysical Journal, 517, 565
- Poisson, E., & Will, C. M. 2014, Gravity: Newtonian, Post-Newtonian, Relativistic (Cambridge University Press)
- Reid, M. J., Menten, K. M., Brunthaler, A., et al. 2014, The Astrophysical Journal, 783, 130
- Riess, A. G., Filippenko, A. V., Challis, P., et al. 1998, The Astronomical Journal, 116, 1009
- Rubin, V. C., Burstein, D., Ford, W. K., J., & Thonnard, N. 1985, ApJ, 289, 81
- Sofue, Y. 1999, PASJ, 51, 445
- Sofue, Y., & Rubin, V. 2001, ARA&A, 39, 137
- Trimble, V. 1987, ARA&A, 25, 425